Journal de la Société Chimique de Mauritanie
Journal of the Mauritanian Chemical Society

Few-layered graphene synthesis by arc-discharge method

Aichata Kane[1,2], Aliou Hamady Barry[2], Salim Mourad Chérif[1], Samir Farhat[1]

[1] *Université Sorbonne Paris Nord, Laboratoire des Sciences des Procédés et des Matériaux, CNRS, LSPM-UPR 3407, F-93430, Villetaneuse, France*
[2] *Département de Chimie, Faculté des Sciences et Techniques de l'Université de Nouakchott AL-Assriya, Mauritanie*

Infos	Abstract - Résumé
	Few layered graphene sheets were synthesized by the electric arc method by sublimation of graphite in helium used as a buffer gas. The arc was created between two graphite electrodes subjected to a continuous electric current. Experiments were designed and conducted by careful control of the turbulent flow leaving radially from a very small inter-electrode space. The graphene obtained was characterized by Raman spectroscopy and by X-ray diffraction. Du graphène de quelques feuillets d'épaisseur a été synthétisé par la méthode de l'arc électrique par sublimation du graphite dans de l'hélium utilisé comme gaz tampon. L'arc a été créé entre deux électrodes en graphite soumises à un courant électrique continu. Les expériences ont été conçues et réalisées en contrôlant soigneusement l'écoulement turbulent partant radialement de l'espace entre les électrodes. Le graphène obtenu a été caractérisé par spectroscopie Raman et par diffraction aux rayons X.

1. INTRODUCTION

Graphene was first isolated by Geims and Novosolev in 2004[1] and has attracted a lot of attention due to its extraordinary properties [1,2]. These unique properties make graphene a valuable building block for an extensive potential application in many areas as in electronics, sensing, energy storage, photonics and optoelectronics. Consequently, a large scale production and high quality of graphene become essential. In this direction, many synthesis methods have been proposed, including micromechanical cleavage of highly ordered pyrolytic graphite (HOPG) [1], chemical exfoliation [3-5], liquid phase exfoliation [6], graphite oxide reduction [7], epitaxial growth on single-crystal silicon carbide SiCby vacuum graphitization [8,9], chemical vapour deposition (CVD) [10,11] and arc discharge [12,13]. Among the above methods, the arc-discharge has unique advantage due to its low cost and the environmentally friendly behaviour since arc does not generate any by-products of toxic gases or hazardous chemicals. The process appears simple, but obtaining high yields of graphene is difficult and requires careful control of experimental conditions. Also, contrarily to nanotubes, graphene synthesis does not require the use of any metal catalyst; the process is timesaving and in one step. Hence, few layer graphene with high quality can be synthesized in large scale and at low cost.The first synthesis of graphene flakes by the arc-discharge method was reported in 2009 by Subrahmanyam *et al.* [12,13] who used graphite sublimation under hydrogen. The resulting graphene was between 2 and 4 layers with small flakes sizeand low quality evidenced by the low Raman ratio intensities I_G/I_Das well as a broad 2D peak in the Raman spectrum. Wu *et al.* have used CO_2 as reactive gas mixed with He in the arc discharge [14]. The obtained graphene sheets were formed by several layers in a gram

Parameters	Values
Cathode	27 mm × 20 mm length
Anode	6.15 mm × 75 mm length
Applied Current	120 A
Voltage	38 V
Gap	3 mm
Buffer gas	He (530 mbar)
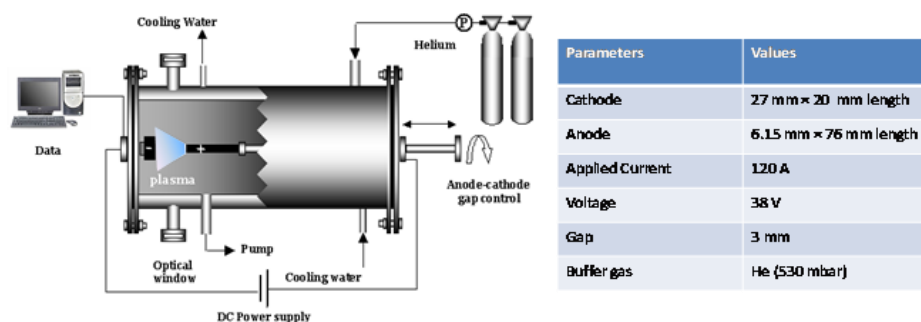
Figure 1. Diagram showing the arc discharge reactor and the experimental parameters used for graphene synthesis.

scale but the structural quality remains low. It has been reported that the presence of H_2 during the arc discharge process terminates the dangling carbon bonds with hydrogen and prevents the formation of closed structures, such as rolling of sheets into nanotubes and graphitic polyhedral particles [15,16].In this direction, Shen *et al.*[17] used three buffer gases namely (H_2-He), (H_2-N_2-He) and (N_2-He), in order to prepare better quality graphene sheets from natural graphite. From their results, it appears that H_2 plays a key role in the formation of graphene sheets. The graphene sheets obtained under (H_2-He) have less layer number than the other buffer gases, leading to the conclusion that more wrinkles and edges would be appeared in this sample. As a result, lower ratio of I_G/I_D was observed. To understand the growth mechanism leading to few-layered graphene by arc discharge in the presence of reactive gas, Qin *et al.*[18] carried out graphene synthesis in pure He, oxidative He (O_2-He) and reductive (H_2-He) buffer gases. They showed that only compact and/or enclosed carbon materials have been produced in inert He buffer gas and that few-layered graphene can only be produced under the atmosphere that contains reactive molecules including H_2, O_2, CO_2, or NH_3[18]. Tan *et al.* [19] reported on multilayer graphene synthesis in a semi-opened arc-discharge plasma reactor. They used different sizes of graphite rods as carbon sources that were vaporized in argon. More recently, Wang *et al.* [20], used a magnetically rotating arc plasma to investigate the effects of buffer gases on graphene flakes synthesis. Few layer graphene were prepared in Ar, He, Ar-H_2, and Ar-N_2 *via* propane decomposition. In this paper, we attempted to synthesize few-layered graphene in arc discharge apparatus under helium as buffer gaswithout using a magnetic field or reactive gases. The arc vaporizes graphite anode in a background gas of helium. This vapour flowing from a sufficiently narrow arc gap can be idealized as a turbulent jet subjected to chemical reactions and grapheme is thought to precipitate along flow streamlines. Experiments were designed and conducted by careful control of experimental conditions. Raman spectroscopy and X-ray diffraction (XRD) are employed to analyse the microstructure of the products. Based on product characterization, graphene formation is discussed.
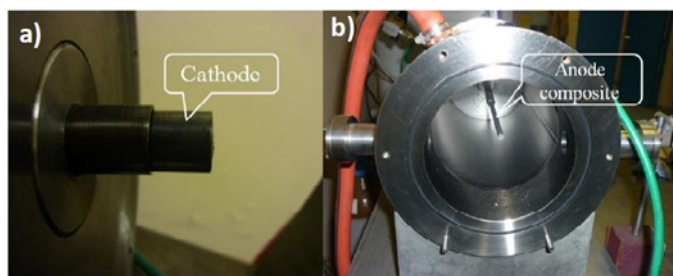
Figure 2. Photography showing the two electrodes.
a) Cathode in graphite. b) Removable composite anode in graphite filled with graphite powder.

2. EXPERIMENTAL

2.1. Synthesis

In the present work, we extend the arc discharge method used earlier in our group for nanotube synthesis [21-23] to the production of graphene (Gr). The reactor chamber consists of a water-cooled stainless steel with two cooled electrode as shown in Figure 1. Both the electrodes were in graphite, one fixed (cathode) and the second movable (anode) (Figure 2). The cathode is made in pure graphite with surface area of 5.7 cm^2. The movable anode is a graphite rod with external diameter of 6.15 mm and surface area of 0.3 cm^2 with a hole of 3 mm in diameter and 30 mm of length, which was filled with graphite powder. A direct current arc discharge was carried out in the reactor chamber filled with pure inert helium (He) as buffer gas. The pressure was kept constant at 530 mbar, and a direct current of 120 A was applied. The plasma was first ignited by contact between the cathode and the anode, which raises the temperature of the contact point until the anode material evaporates. Indeed, the anode is the most thermally loaded electrode. Therefore, it ablates due to excessive heating from the plasma. Anode ablation induces the formation of carbon atoms, molecules and ions. The elevated temperature (~4000 K) caused continuous evaporation of the anode material with turbulent flux and vortices. Then the anode was manually moved toward the cathode in order to continually adjust the desired distance between the electrodes fixed here at 3 mm. This narrow gap allows efficient mixture of carbon vapour with helium atmosphere thereby improving graphene yield. The most stable and high yield arc process requires a stable arc current and hence plasma for the duration of synthesis. The plasma was observed through a quartz window in the reaction chamber. A magnified image of the luminescent plasma was projected from this window on a screen and allowed to carefully adjust the distance between the anode and the cathode during the experiment.

2.2. Characterization

We used Raman spectroscopy (HR800, HORIBA Jobin-Yvon) working in a confocal mode in air and with the back-scattering configuration, 632.8 nm laser excitation, to identify crystalline quality and graphene thickness. The X-Ray diffraction XRD analysis was performed using 2INELTM diffractometers with Co-Kα radiation.

3. RESULTS AND DISCUSSION

In our experiment, a high current-low voltage DC power supply was used in which current was fixed at 120 A. Since, the key aspects defining graphene properties are the atomically-organized crystallite size and the grain boundaries structure, which could be obtained through Raman and XRD analysis of the collected samples. In Figure 3, different locations are sampled in order to reliably describe the sample. Raman spectroscopy is a powerful technique which can be used to characterise the structural properties of graphene. The main features in the graphene Raman spectra are peaks D (~1333 cm^{-1}), G (~1580 cm^{-1}) and 2D (~2660 cm^{-1}), in correspondence with Raman shifts. The D' peak (~1620 cm^{-1}) originate from intra-
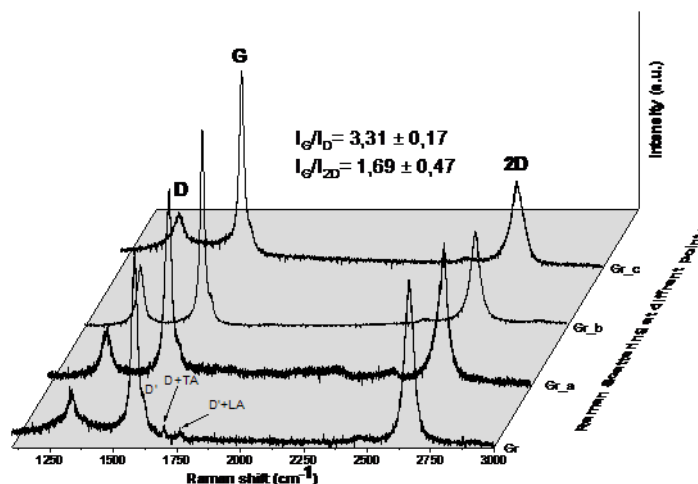
Figure 3. Raman spectra of the synthesized graphene in helium arc discharge method scattered at different locations.

valley one-phonon and is caused by disordered structure of graphene. Hence both D and D' peaks, require a defect to be activated [24-26]. Graphene edges also constitute a kind of defect due to the broken in translational symmetry. Besides the peaks D, D', G and 2D, other weak Raman modes can also be observed including D'+TA and D'+LA in the range 1700-1750 cm^{-1}. They originate from phonon dispersion of in-plane longitudinal acoustic (LA) and transverse acoustic (TA) branches [24]. The intensity of the D-band is directly proportional to the level of defects in the sample. The G band corresponds to the zone-center E_{2g} mode related to phonon vibrations in sp^2 carbon domains and is related to the tangential elongation modes in graphene [27,28]. It is almost identical regardless of the number of sheets. Finally, 2D band which is the second order of the D band does not need to be activated by the proximity of a defect. As a result, it is always a strong band in graphene, and it is used to determine the number of layer of the graphene. The 2D band is caused by the second-order zone boundary phonons and it's very sensitive to the number of layers in the graphene.The G-band has been used as a characteristic band for ordered graphite carbon sheets [28]. The intensity ratio of the G band to the D band I_G/I_D is used to characterize the structural quality of graphitic materials [29]. Higher I_G/I_D ratio indicates higher crystal quality. Finally, since most of the potential applications of graphene are dependent on large area sample production, a theoretical model supported by experimental results was proposed to correlate the I_G/I_D ratio between the C-C stretching (G band) and the defect-induced (D band) modes with the crystallite sizes only for samples with sizes larger than the phonon coherence length, which is found equal to 32 nm [30]. Hence, Raman spectroscopy could be proposed as a quick technique to measure the in plane crystallite size (L_a) of nanostructured graphitic samples using the following equation, where λ is the laser excitation in (nm) [31].

$$L_a(nm)= (2.4\times10^{-10})\lambda^4 \ (I_D/I_G)^{-1} \tag{1}$$

In two-dimensional (2D) carbon sp^2 honeycomb lattices, defects can be either zero-dimensional (0D), such as vacancies or dopants or one-dimensional (1D), such as dislocations or crystallite borders [32]. The I_G/I_D ratio shows the presence of defects, which can originates from structure defect or the presence of edges or more wrinkles [17].In addition, structural amorphization could lead to horn-shaped sheath aggregate of graphene down to more complex structures. In the arc discharge, the complex chemical mixture of species and spatiotemporal variations of process parameters can change from one experiment to the other. As shown table1, the average I_G/I_D ratio is 3.31 ± 0.17which is comparable to the graphene obtained by Shen *et al.*[29] (I_G/I_D=2.25) in a mixing atmosphere of (He-Ne). By applying equation (1), we estimated the average in plane crystallite size (L_a) of nanostructured graphitic to 127±7 nm. The position of the 2D band and the ratio between the G band to the 2D band provides information on the layers number that contains the graphene sheets [33]. Thus, the number of layers could be estimated to less than 5 layers according to the position of 2D band [34]. Also, based on the I_G/I_{2D} ratio we obtained values of ~1.70 ± 0.47 comparable of CVD grown graphene (I_G/I_{2D}) ~1.3 [35].

To further confirm graphene phase and morphology, X-ray diffraction was taken in 2θ angle range from 20° to 120°. Figure 4 shows a typical XRD pattern comparable to the XRD pattern reported by Li *et al* [34] and Karmakar *et al.* [36] indicating a good degree of purity that verify the crystallinity of our product. The sharp and high peak (002) at 2θ= 30.51 indicates a highly organized crystal structure with an interlayer

Tableau 1 : Résultats de la synthèse des complexes **1-9.**

Position	D band (cm^{-1})	G band (cm^{-1})	2D band (cm^{-1})	I_G/I_D	I_G/I_{2D}	La (nm)
Gr	1335	1585	2667	3.49	1.14	134
Gr_a	1335	1579	2658	3.22	1.34	124
Gr_b	1320	1564	2638	3.06	2.02	118
Gr_c	1331	1575	2660	3.45	2.28	132
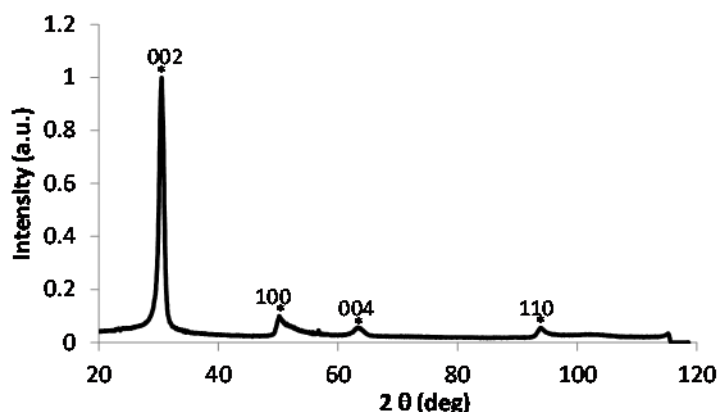
Figure 4. X-ray diffraction patterns of (Gr) sample synthesized with Cobalt-Kα radiation (λ=1.7889 Å).

distance of 0.34 nm which is almost the same distance between the layers in the graphite. The secondary reflections at 2θ of ~50.3°, ~63.4° and ~93.8° was indexed as (100), (004) and (110) crystal planes of graphite respectively as reported in the Joint Committee on Powder Diffraction Standards database (JCPDS -01-075-1621).

As schematically depicted in Figure 5, graphene rich material is thought to condense from vaporized small carbon species C, C_2, C_3 etc..… formed in the plasma. Indeed, the temperature T_0 in the arc is higher than 10,000 K as calculated by modelling [21] and confirmed by optical emission spectroscopy measurements. The mixed carbon species then condenses into the product by cooling while mixing with helium and moves away from the central plasma zone to the water-cooled cathode and reactor walls and deposits on them. This leads to a high quench rates and high levels of super cooled and supersaturated vapour with graphene formation. One can model the chemical processes taking place in a turbulent fan jet leaving radially from a very small inter-electrode space in graphene conditions. The turbulent jet model accounts for the main processes controlling graphene formation in electric arcs, namely, (i) cooling and mixing of carbon vapour in a buffer gas, (ii) reactions of cluster growth and decomposition under non-isothermal conditions, (iii) formation of soot particles and heterogeneous reactions on their surface.
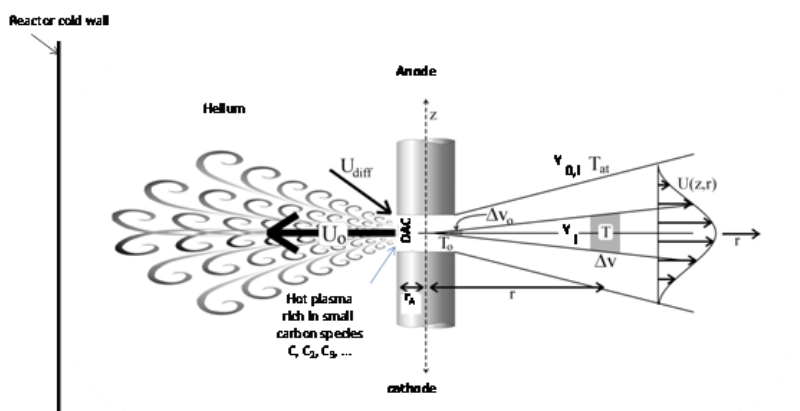
Figure 5. Scheme explaining a possible growth mechanism of graphene in arc-discharge.

The model solves the gas dynamic equations governing the jet expansion of an initial volume ΔV_0 rich in carbon at the temperature T_0 with a high initial velocity U_0 into the surrounding pure and cold helium gas at T_{at}. As schematically drown in Figure 5 (right part), velocity profile $U(z,r)$ in the plane (z,r) represents a jet cross section with a parabolic and symmetric form. Work is in progress to simulate the expansion process in the specific conditions of graphene synthesis by arc discharge.

4. CONCLUSIONS

In this work, it was confirmed by Raman and XRDanalysis that few-layers graphene were successfully produced by arc discharge method under helium gas by using graphite powder as carbon source. The relatively weak Raman peak D and the sharp and near-symmetric peak 2D, attest that a reasonable quality of few-layer graphene was achieved. There is still no common theory describing the exact mechanism of graphene formation in the arc, but this simple process have several advantages as a high gas temperature capable of dissociating easily graphite, a relatively high concentration of small carbon radicals in the gas phase and extremely high quenching rates. For the synthesis of graphene, it will be necessary to minimize the formation of the deposit while increasing the flow of species out of the plasma column. The anode is first moved back to obtain vortices, then gradually brought closer to the cathode at the desired distance between the electrodes while maintaining a turbulent regime to improve the flux of C_2 outside the plasma column. With our apparatus we have obtained graphene with good lattice structure and quality without using any catalyst or any active gas like N_2, H_2, CO_2 or NH_3.While graphene growth mechanism is not yet clearly elucidates, calculated flow and trajectories in our conditions attest of a fully turbulent jet in the narrow arc gap with vortices around the electrodes that controls graphene formation in the arc-discharge.

REFERENCES

[1] K.S. Novoselov, A.K. Geim, S.V. Morozov, D. Jiang, Y. Zhang, S.V. Dubonos, I.V. Grigorieva, A.A. Firsov, *Science,* 306 (2004) 666.
[2] K.S. Novoselov, Z. Jiang, Y. Zhang, S.V. Morozov, H.L. Stormer, U. Zeitler, J.C. Maan, G.S. Boebinger, P. Kim, A.K. Geim, *Scienc.,* 315 (2007) 1379.
[3] S. Stankovich, D. A. Dikin, R. D. Piner, K. A. Kohlhaas, A. Kleinhammes, Y. Jia, Y. Wu, S.T. Nguyen, R. S. Ruoff, *Carbon,* 45 (2007) 1558–1565.
[4] H. C. Schniepp, J. L. Li, M. J. McAllister, H. Sai, M. Herrera-Alonso, D. H. Adamson, R. K.; Car, R. Prud'homme, D. A. Saville, I. A. Aksay, *J. Phys. Chem. B.,* 110 (2006) 8535–8539.
[5] X. L. Li, X. R. Wang, L. Zhang, S. W. Lee, H. J. Dai., *Science,*319 (2008) 1229–1232.
[6] Y. Hernandez, V. Nicolosi, M. Lotya, F. M. Blighe, Z. Sun, S. De, I. T. McGovern, B. Holland, M. Byrne, Y. K. Gun'Ko, J. J. Boland, P. Niraj, G. Duesberg, S. Krishnamurthy, R. Goodhue, J. Hutchison, V. Scardaci, A. C. Ferrari & J. N. Coleman, *Nat. Nanotechnol.,* 3 (2008) ,563.
[7] V.C. Tung, M.J. Allen, Y. Yang, R.B. Kaner, *Nat. Nanotechnol.,* 4 (2009), 25.
[8] P. Sutter, J.I. Flege, E. Sutter, *Nat. Mater.,* 7 (2008), 406–411.
[9] C. Berger,Z. M. Song, X. B.Li, X. S. Wu, N. Brown, C. Naud, D. Mayou, T. B. Li, J. Hass, A. N. Marchenkov, E. H. Conrad, P. N.First, W. A. de Heer, *Science,* 312 (2006), 1191–1196.
[10] S. J. Chae, F.Güneş, K. K. Kim, E. S. Kim, G. H. Han, S. M. Kim, H. J. Shin, S. M. Yoon, J.Y. Choi, M.H. Park, C. W. Yang, D. Pribat, and Y. H. Lee, *Adv. Mater.,* 21 (2009), 2328-2333.
[11] X. S. Li, W. W. Cai, J. H. An, S. Kim, J. Nah, D. X. Yang, R. Piner, A. Velamakanni, I. Jung, E. Tutuc, S. K. Banerjee, L. Colombo, *Science,* 324 (2009), 1312–1314.
[12] L. S. Panchakarla, K. S. Subrahmanyam, S. K. Saha, Achutharao Govindaraj, H. R. Krishnamurthy, U. V. Waghmare, and C. N. R. Rao, *Adv. Mater.,* 21 (2009), 4726–4730.
[13] K. S. Subrahmanyam, L. S. Panchakarla, A. Govindaraj and C. N. R. Rao, *J. Phys. Chem. C.,* 113 (2009) 4257.
[14] Y. P. Wu, B. Wang, Y. F. Ma, Y. Huang, N. Li, F. Zhang and Y. S. Chen, *Nano Res.,*3 (2010) 661.
[15] X.K. Wang, X.W. Lin, M. Mesleh, M.F. Jarrold, V.P. Dravid, J.B. Ketterson, R.P.H. Chang, *J. Mater. Res.,* 10 (1995) 1977.
[16] X.K. Wang, X.W. Lin, V.P. Dravid, J.B. Ketterson, R.P.H. Chang, *Appl. Phys. Lett.,* 66 (1995) 2430.
[17] B. Shen, J. Ding, ,X. Yan, W. Feng, J. Li, Q. Xue, *Applied Surface Science,* 258 (2012) 4523-4531.
[18] B. Qin, T. Zhang, H. Chen,Y. Ma, *Carbon,* 102 (2016) 494-498.

[19] H. Tan, D. Wang, Y.Guo, *Materials*,12 (2019), 2279.

[20] C. Wang, M. Song, X. Chen, D. Li, W. Xia, *Nanomaterials*,10 (2020), 309.

[21] S. Farhat and C. Scott "J.*Nanosci.and Nanotech*., 6 (2006) 1189-1210 .

[22] I. Hinkov, S. Farhat and C. D. Scott *Carbon*, 43 (2005) 2453-2462.

[23] S. Farhat, M. Lamy de La Chapelle, A. Loiseau, C. D. Scott, S. Lefrant, C. Journet and P. Bernier*, J. Chem Phys*., 15 (2001) 6752-6759.

[24] P. H. Tan, C. Y. Hu, J. Dong, W. WanCi Shen, B. Zhang*Phys. Rev. B*, 64, (2001) 214301.

[25] J. Kastner, T. Pichler, H. Kuzmany, S. Curran, W. Blau, D. N. Weldon, M. Delamesiere, S. Draper, H. Zandbergen, *Chem. Phys. Lett*., 221 (1994) 53–58.

[26] C. Casiraghi, A. Hartschuh, H. Qian, S. Piscanec, C. Georgi, A. Fasoli, K. S. Novoselov, D. M. Basko, A. C. Ferrari, *Nano Lett*., 9 (2009) 1433–1441.

[27] K. S. Subrahmanyam, S. R. C. Vivekchand, A. Govindaraj, , C. N. R. Rao, *J. Mater. Chem.,*18 (2008) 1517-1523.

[28] E.K. Athanassiou, R. N. Grass, W. J. Stark, *Nanotechnology.,* 17 (2006) 1668–1673.

[29] J. Shen, T. Li, Y. Long, M. Shi, N. Li, M. Ye, *Carbon.,* 50 (2012) 2134-2140.

[30] J. Ribeiro-Soares, M.E. Olivero, C. Garin, M.V. David, L. G. P. Martins, C. A. Almeida E. H. Martins-Ferreira, K. Takai, T. Enoki, R. Magalhães-Paniago, A. Malachias, A. Jorio, B.S. Archanjo, C. A. Achete, L. G. Cançado, *Carbon,* 95 (2015) 646.

[31] A. Jorio, M.A. Pimenta, *Carbon*, 46 (2008) 272.

[32] L. G. Cançado, M. G. da Silva, E. H. M. Ferreira, F. Hof, K. Kampioti, K. Huang, A. Pénicaud, C. A. Achete, R. B. Capaz and A. Jorio, *Mater.*,4 (2017) 025039.

[33] A. C. Ferrari, J. C. Meyer, V. Scardaci, C. Casiraghi, M. Lazzeri, F. Mauri, S. Piscanec, D. Jiang, K. S. Novoselov, S. Roth, A. K.Geim, *Phys. Rev. Lett,.*97 (2006), 187401.

[34] Z.Q. Li, C.J. Lu, Z.P. Xia, Y. Zhou, Z. Luo, *Carbon,* 45 (2007) 1686–1695.

[35] A. Reina, X. T. Jia, J. Ho, D. Nezich, H. B. Son, V. Bulovic, M. S. Dresselhaus, J. Kong, *Nano Lett*., 9 (2009) 30-35.

[36] S. Karmakar , A. B. Nawale , N. P. Lalla , V. G. Sathe , S. K. Kolekar , V. L. Mathe , A. K. Das , S. V. Bhoraskar, *Carbon*, 55 (2013) 209-220.